

S2-3 Free Tropospheric Aerosols Backscatter, Depolarization Ratio and Humidity as Derived from Raman Lidar Observations

Tetsu Sakai, Takashi Shibata, Soung-An Kwon, Yoon-Suk Kim, Koichi Tamura, and Yasunobu Iwasaka
 Solar-Terrestrial Environment Laboratory, Nagoya University
 Furo-cho, Chikusa-ku, Nagoya 464-8601, Japan
 Phone: 052-789-4317, FAX: 052-789-4301, E-mail: tetsu@stelab.nagoya-u.ac.jp

1. Introduction

Free tropospheric aerosol particles are frequently transported long distances and can affect remote areas. The transport of mineral dust particles, which originate from the arid and semi-arid lands of the Asian Continent, to the North Pacific region has been studied for over twenty years. In addition to these natural aerosols, there is concern over the influence of anthropogenic aerosols from Asian industrial regions on the tropospheric chemistry in the Pacific region.

Since the aerosol properties such as size, phase, shape and chemical composition critically depend on the ambient relative humidity, it is important to measure aerosol properties with the relative humidity in their natural state. Raman lidar has been developed to remotely measure the vertical profiles of humidity and aerosol optical properties simultaneously (Whiteman et al., 1992; Ansmann et al., 1992; Shibata et al., 1996; Sakai et al., 1997). Depolarization ratio is a useful parameter for the study of aerosol microphysics as well as the aerosol backscattering and extinction coefficients obtainable with the lidar, because deviations from zero can indicate particle nonsphericity. The particle shape critically controls the particle's optical properties and hence affects radiative processes as well as the vertical distribution of the particles.

We investigated the seasonal and altitude characteristics of the aerosol backscattering and the depolarization ratio in relation to the relative humidity in the free troposphere on the basis of Raman lidar observations at Nagoya, Japan (35.1°N, 137.0°E) from March 1994 to February 1997. Backward trajectory analyses were performed to investigate the relation between the aerosol optical properties and the transport pathways from the source areas.

2. Measurement

The Raman lidar system is on the campus of Nagoya University in an urban area located 20 km north of the Ise Bay and 70 km inland from the Pacific Ocean. Specifications of the lidar system are listed in Table 1. More details are given by Shibata et al. (1996). Three wavelengths of Nd:YAG laser are vertically transmitted into the atmosphere and the backscattered light from atmospheric gases and aerosol particles is collected with a Cassegrain telescope. The light is separated into five

spectral components and simultaneously detected with five photomultiplier tubes (PMTs). During normal operation, the signals are recorded with a vertical resolution of 50 m (30 m after April 1996) for thirty minutes. We smoothed the data to 350 m (330 m after April 1996) in the analyses to improve the signal to noise ratio.

The measurements were carried out in the nighttime under mostly cloud-free conditions. A total of 332 tropospheric profiles were taken during the period of March 1994 to February 1997.

Table 1 Specifications of the Raman lidar at Nagoya University (35.1°N, 137.0°E)

Transmitter:		
Laser type	Nd:YAG	
Wavelength (nm)	355, 532, 1064	
Energy/pulse (mJ)	200, 50, 430	
Repetition rate (Hz)	10	
Beam divergence (mrad)	0.2 (after collimator)	
Receiver:		
Telescope type	Cassegrain	
Diameter (m)	1.0	
Field of view (mrad)	1.5	
Detector	PMT (HAMAMATSU R331, R1767)	
Signal detection	Photon counting	
Range resolution (m)	50 (30 after April 1996)	
Detected wavelengths (nm) and species	407.5	Raman water vapor
	375.4	Raman oxygen
	532 //, ⊥	Mie/Rayleigh, polarization
	1064	Mie/Rayleigh

3. Results

3.1 Vertical distributions of aerosol backscattering, depolarization ratio and humidity

Fig. 1 shows the vertical profiles of the backscattering ratio (R) and aerosol depolarization ratio ($\delta_a = \perp / (// + \perp)$) at the wavelength of 532 nm, water vapor mixing ratio (w), and relative humidity (RH) measured with the Raman lidar on April 21 and July 23, September 11 and December 23 in 1994, which represent the seasonal characteristics. Relative humidity is calculated from the observed water vapor mixing ratio combined with the temperature and pressure data obtained with the coincident radiosonde or the global objective analysis data supplied by the Japan Meteorological Agency. The humidity and temperature profiles obtained with the coincident radiosonde are also

shown in Fig. 1c. Also shown the 5-day isentropic backward trajectories arriving at the lidar site at the altitudes of 3 km and 6 km.

Large aerosol backscattering ratios, R , were found in the spring season (Fig. 1a), with peaks at 2.3 km, where R was 5.2, and between 4 and 6 km, where R was about 2.4. The aerosol depolarization ratios between 4 and 8 km were high, about 25%, indicating a substantial amount of nonspherical particles in this region. The presence of dust particles is probable because the relative humidities were less than 20% in this region. The backward trajectories indicated that the air parcels had been carried over the Asian Continent by a westerly flow. Some air parcels at 6 km showed cyclonic motion associated with frontal activity at around 45°N, 75°E. In this area, from eight to thirty-two occurrences of dust rises were reported in the spring of 1994.

Figure 1b shows the profiles observed in the summer when a Pacific high pressure system covered the northwestern Pacific region. The values of R were small (average 1.06) and nearly constant between 2 and 10 km. The aerosol depolarization ratios in this region had low values of about 4%, indicating the

predominance of spherical, near spherical, or small ($r < \lambda$) particles. A relatively large amount of water vapor was observed between 0.5 and 10 km and the mixing ratios approximately linearly decreased with height up to 6.5 km. The air parcels at both altitudes had passed slowly over the Pacific Ocean.

The autumn profiles (Fig. 1c) showed steep vertical gradients of humidity (w and RH) and δ_a at 4.0 km. We measured values of δ_a less than 2% with high RH values between 70 and 90% below 4.0 km. The aerosol depolarization ratios sharply increased to 17% and the RH decreased to as low as 2% at an altitude between 3.6 and 4.0 km, where the temperature inversion was present. The backward trajectories for the two altitudes showed different pathways: the air parcels present at 3km had passed over the Pacific Ocean while those at 6 km had been carried over the Asian Continent. This vertical structure (sharp increase in δ_a and decrease in w (RH) with height) has been frequently observed between 2 and 4 km throughout the year except for the summer. This structure can be seen in Fig. 1a at 3 km.

Figure 1d shows the profiles observed in the winter, when a strong cold front had just passed the lidar site.

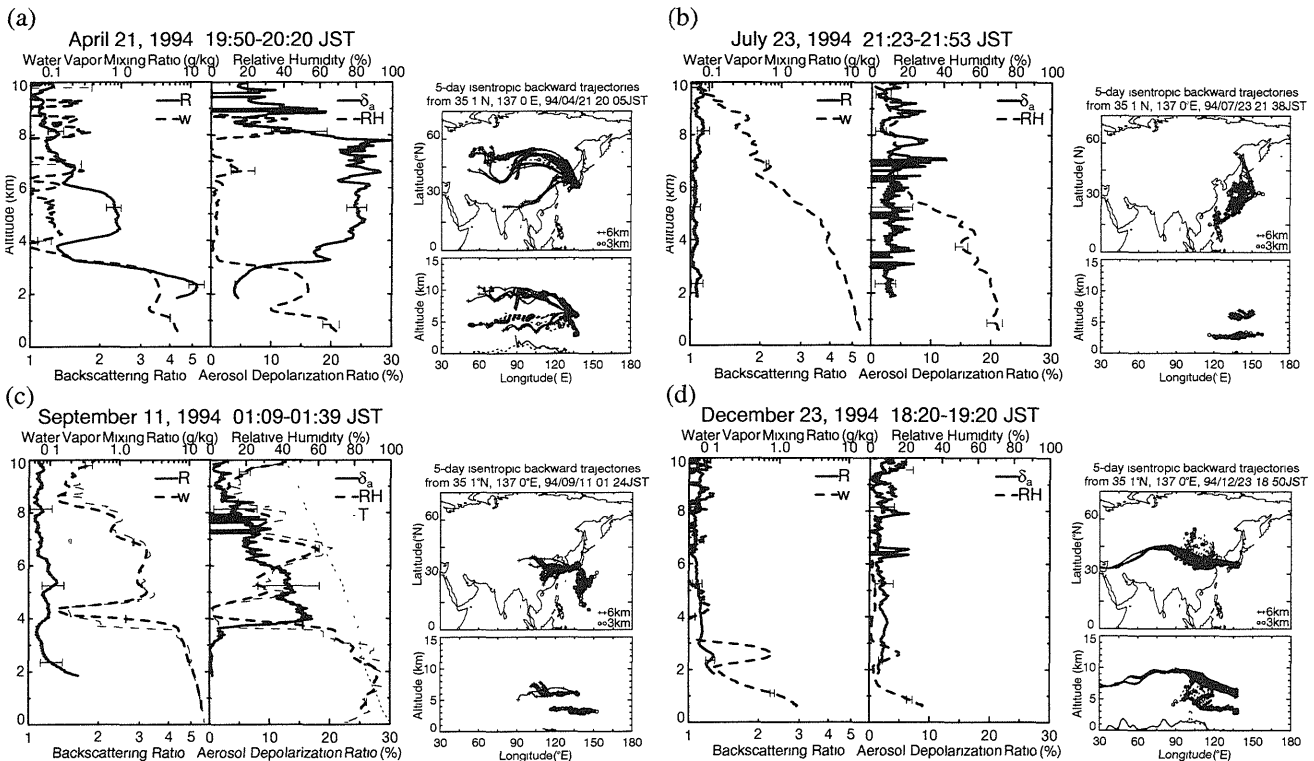


Fig. 1 Vertical profiles of backscattering ratio (R) and aerosol depolarization ratio (δ_a) at 532 nm, water vapor mixing ratio (w) and relative humidity (RH) obtained with the Raman lidar at Nagoya (35.1°N, 137.0°E) and the horizontal and vertical cross sections of 5-day isentropic backward trajectories arriving at the lidar site on (a) April 21, (b) July 23, (c) September 11, and December 23, 1994. Thin lines in Fig. 1c shows the temperature and humidity profiles obtained with the coincident radiosonde. Temperature scale is 200-300 K.

The average of R was 1.1 and that of δ_a was 2% between 2 and 10 km. The relative humidity was low (<20%RH) above 2 km. The air parcels at 3 km had been carried over the Asian Continent in the middle-upper troposphere and those at 6 km had moved through the upper troposphere (6-10 km) at a mean speed of 30 m s^{-1} , driven by jet streams.

3.2 Aerosol depolarization ratio as a function of relative humidity

Figure 2 shows the scatter plots of the aerosol depolarization ratio versus the relative humidity between 2 and 8 km observed for the period March 1994 to February 1995. The data are plotted with different symbols for the two altitude regions (2-4 km and 4-8 km) in each season. Seasonal and altitude dependencies of the distributions were found in Fig. 2. Aerosol depolarization ratios as high as 25% were observed frequently in the 2-8 km region in the spring (MAM) and in the 4-8 km regions in the autumn (SON) and winter (DJF) (Fig. 2a, 2c, and 2d). It should be noted that these high δ_a values were found in moist regions with RH as high as 80% at 4-8 km regions in the spring and autumn, suggesting that the particles mainly consisted of water-insoluble substances (e.g., mineral dust) that existed as solid crystal in the moist air (type (a) in Fig. 3).

The distribution pattern of δ_a as a function of RH in the summer (JJA) and 2-4 km region in the autumn (Fig. 2b and 2c) showed typical characteristics; they generally showed low δ_a values (<5%) over a wide range of RH and showed high δ_a values (>10%) only where the RH was less than about 50%. Since the air parcels in these regions had mainly passed over the Pacific Ocean, these characteristics might be due to the predominance of maritime aerosols (e.g., sea-salt) that exhibits the properties of deliquescence and efflorescence (type (b) in Fig. 3); they existed as solid crystals and thus indicated high δ_a values in the dry air (below the RH for deliquescence or efflorescence depending on the history of RH), whereas they existed as aqueous solution droplets and indicated low δ_a values in the moist air. For example, the efflorescence and deliquescence points of NaCl particles at 298 K are 46-48% and 75% and those of $(\text{NH}_4)_2\text{SO}_4$ particles are 37-40% and 80%, respectively (Tang, 1996).

It must be noted that the value of δ_a measured with the lidar is averaged temporally (~30 minutes) and vertically (over 330-350 m) so that if several kinds of particles with different δ_a values coexist in the air, the value indicates the average weighted by the particle's backscattering cross section.

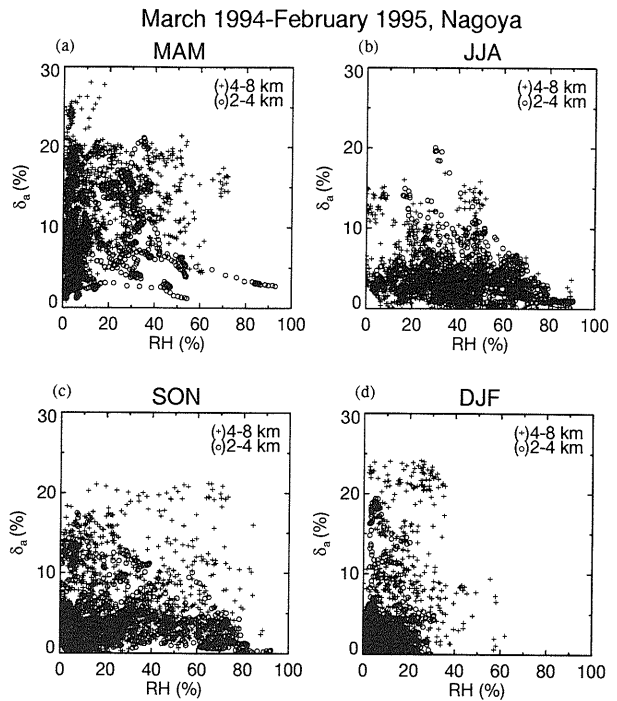


Fig. 2 Aerosol depolarization ratio (δ_a) as a function of relative humidity (RH) between the altitude ranges of 2-4 km (○) and 4-8 km (+) obtained with the Raman lidar for the periods (a) March to May, (b) June to August, (c) September to November, and (d) December to February in 1994-1995.

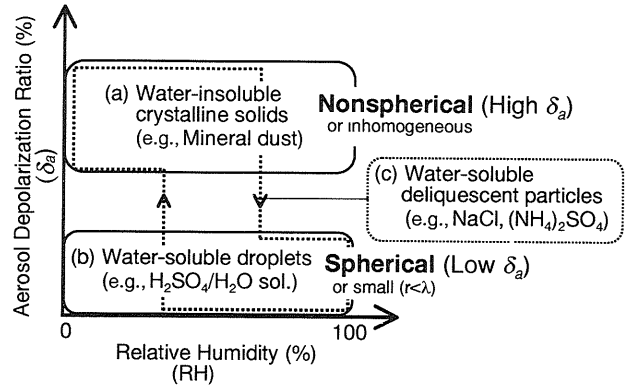


Fig. 3 Schematic diagram of the relationship between aerosol depolarization ratio (δ_a) and relative humidity (RH) for three aerosol types: (a) water-insoluble crystalline solids, (b) water-soluble droplets, and (c) water-soluble particles that have properties of deliquescence and efflorescence.

3.3 Temporal variations of vertically integrated aerosol backscattering coefficient

Figure 4 shows the temporal variation of the vertically integrated aerosol backscattering coefficient (IBC) at 532 nm from March 1994 to February 1997. The value of IBC was calculated separately for two altitude ranges (2-4 km and 4-8 km). We excluded the data that corresponded to saturated conditions ($RH \geq 100\%$) to eliminate the backscattering components of clouds. However, some components of clouds might be included because of uncertainties in the humidity measurements, and because of the temporal and vertical resolution of the data.

A maximum IBC was found in the spring (March–May) with sharp peaks in both altitude regions. The mean IBCs for 2-4 km in this season were 1.64, 1.71, and $2.22 \times 10^{-3} \text{ sr}^{-1}$ for 1994, 1995 and 1996, respectively, which were 1.6-2.2 times larger than the annual mean. For 4-8 km, the IBCs in this season were 1.43, 1.28, and $1.42 \times 10^{-3} \text{ sr}^{-1}$ for the three years, respectively, which were 1.6-1.8 times larger than the annual mean. These peaks were probably due to the Asian dust particles, because maximum occurrence of dust rises were reported in the Asian arid region in this season and because most of the air parcels over the lidar site were passed over the Asian Continent.

A second IBC maximum was found at 2-4 km in July–August (lower panel in Fig. 4), in which the mean IBC was $0.76\text{--}1.64 \times 10^{-3} \text{ sr}^{-1}$. This second maximum was not found at 4-8 km. The air parcels were mostly passed over the Pacific Ocean in this season.

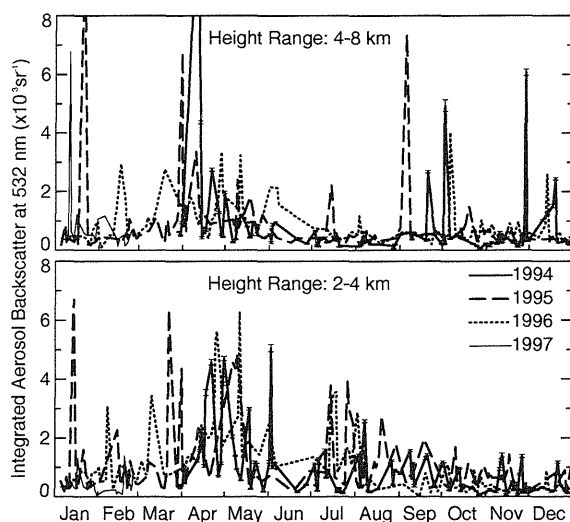


Fig. 4 Temporal variation of vertically integrated aerosol backscattering coefficient at 532 nm obtained with the Raman lidar at Nagoya from March 1994 to February 1997. The height ranges of the integration are 4-8 km (upper panel) and 2-4 km (lower panel), respectively.

4. Summary

Our results suggest that the transport pathways from the source areas (the Asian Continent and the Pacific Ocean) and the ambient relative humidity critically control the aerosol depolarization ratio in the free troposphere over Nagoya. However, coincident measurement and comparison of lidar and in situ sampling data are indispensable for an interpretation and application of the lidar data that clarifies the physical and chemical characteristics of the free tropospheric aerosols.

References

- Ansmann, A., Riebesell, M., Wandinger, U., Weitkamp, C., Voss, E., Lahmann, W., and Michaelis, W. (1992). Combined Raman elastic-backscatter LIDAR for vertical profiling of moisture, aerosol extinction, backscatter, and LIDAR ratio. *Applied Physics*, B55: 18-28.
- Sakai, T., Shibata, T. and Iwasaka, Y. (1997). Relative Humidity, Backscattering Ratio and Depolarization Ratio as Derived from Raman Lidar Observations. *Journal of the Meteorological Society of Japan*, 75: 1179-1185.
- Shibata, T., Sakai, T., Hayashi, M., Ojio, T., Kwon, S. A., and Iwasaka, Y., (1996). Raman lidar observations: simultaneous measurements of water vapor, temperature and aerosol vertical profiles, Part I. *Journal of Geomagnetism and Geoelectricity*, 48: 1137-1144.
- Tang, I. N. (1996). Chemical and size effects of hygroscopic aerosols on light scattering coefficient. *Journal of Geophysical Research*, 101: 19245-19250.
- Whiteman, D. N., Melfi, S. H., and Ferrare, R. A., 1992. Raman lidar system for the measurement of water vapor and aerosols in the Earth's atmosphere. *Applied Optics*, 31: 3068-3082.